

# Micro encapsulation and characterization of Diclosulam in Xanthan Gum based polymeric system for smart delivery of herbicide in crop production

Original Research Article

## 1 ABSTRACT

2

**Aim:** Micro encapsulation of diclosulam herbicide was done in xanthan gum based polymeric system through ionotropic gelation method to formulate a slow-release herbicide to achieve prolonged weed control in irrigated upland ecosystem.

**Place and duration of study:** The slow-release formulation of diclosulam was synthesized and characterized in the Department of Nano Science & Technology, Tamil Nadu Agricultural University during January to July 2022.

**Methodology:** Xanthan gum- alginate microsphere system was synthesized with varying concentrations of calcium chloride (CaCl<sub>2</sub>) (2, 4 and 6 per cent) to encapsulate diclosulam through ionotropic gelation. The size, entrapment efficiency, pore volume, pore radius, surface area and swelling behavior of microspheres were assessed to achieve higher loading of diclosulam and good stability of microspheres.

**Results:** The mean diameter of xanthan gum-alginate microsphere was higher with 6 per cent ion gelation bath followed by the concentration of 4 and 2 per cent. Higher entrapment efficiency of diclosulam was achieved with loading of two percent diclosulam in six per cent calcium crosslinked microspheres

**Conclusion:** Xanthan gum-alginate microsphere system offers both burst release and controlled release of active ingredients. However, controlled release polymeric templates with herbicide will synchronize the release of herbicide with the emergence of weeds in the cropped situations for better weed management.

3 **Keywords:** *Micro encapsulation, Xanthan gum, Sodium Alginate, Diclosulam, Ion gelation*

## 4 1. INTRODUCTION

5

6 Herbicides are the second-largest category of plant protection chemical behind insecticides  
7 in terms of consumption. The Indian herbicide market had achieved the growth of 12.3 per  
8 cent since 2018, compared to the growth of 8.9 per cent for other insecticide and fungicide.

9 The use of herbicides is the efficient strategy to manage weeds in crop production. However,  
10 the continuous and indiscriminate use of herbicides cause phytotoxicity in crops, faster  
11 degradation due to light, persistence in the soil, and leaching into ground water. Overuse of

12 herbicides affect succeeding crops through the carry over effect in the soil. The development  
13 of herbicide-resistant weed species, and shift in weed flora were observed due to the  
14 frequent use of herbicides to control weeds [1]. Up to 20 to 25 DAS, pre-emergence  
15 herbicides have proven to be very successful, but late-arriving weeds obstruct pegging, pod  
16 development, and harvesting [2]. The fate of herbicides in the soil determines the efficiency  
17 of herbicidal activity, where rapid conversion of intermediates in the soil making less effective  
18 against weeds. In addition, intermediate compounds from the degradation path of herbicides  
19 in soil contaminate the groundwater [3]. Diclosulam (2', 6'-dichloro-5-ethoxy7fluoro [1,2,4]  
20 triazolo[1,5c] pyrimidine2sulfonamide) is a low volume herbicide belonging to sulfonamide  
21 family. Diclosulam interfere with Aceto-Hydroxy Acid Synthase (AHAS), a key enzyme  
22 involved in the synthesis of branched-chain amino acids such as leucine, isoleucine and  
23 valine in plants, thus affecting protein synthesis and cell division that leads to death of  
24 targeted weeds. Diclosulam is recommended as pre-emergence herbicide (soybean,  
25 groundnut, sorghum, potato, maize, wheat, barley and oats), applied at 1 to 3 days after  
26 sowing with the optimum dose of 20 g a.i. ha<sup>-1</sup> for groundnut [2]. Phytotoxicity symptoms  
27 such as yellowing of leaves are reported in groundnut with the application of diclosulam.  
28 Similarly, pre-emergence application of diclosulam controls weeds up to 40 days of sowing in  
29 groundnut which warrants either hand weeding and post emergence application of herbicides  
30 to maintain weed free situation to prevent economic yield loss. Diclosulam binds with soil that  
31 leads to less mobility and leaching in soils causing less herbicidal activity. Hence, the  
32 research was proposed to design diclosulam systems for releasing active molecules at  
33 regulated manner to maintain the concentration of herbicide in soil to cause herbicidal action.

34

35 Encapsulation with natural polymers is the best strategy to improve weed control efficiency of  
36 herbicides and reduce herbicide adsorption in the soil. Microsphere encapsulation of  
37 agrochemicals in pectin based polymeric system was used for the smart release of  
38 herbicides [4]. Diverse properties of natural polymers were preferred for encapsulation of  
39 herbicides over synthetic materials due to non-toxicity in nature, abundance availability and  
40 the cost [5]. Xanthan gum and alginate are natural polymers, explored as a carrier for  
41 encapsulation of plant protection chemicals and microbes. Xanthan gum is a microbial extra  
42 cellular polysaccharide produced by Gram negative aerobic bacteria *Xanthomonas*  
43 *campestris* [6]. Xanthan gum is biocompatible in nature, bio adhesive, biodegradable, non-  
44 toxic and low cost which makes suitable candidate for the encapsulation of agrochemicals  
45 [7]. Biofilms, hydrogels, micro particles and nanoparticle of xanthan gum and xanthan gum  
46 based composites are widely used for designing controlled release systems [8]. Xanthan  
47 gum acts as emulsifier and thickening agent besides its good water-control properties and

48 pseudoplastic behavior, where xanthan gum at lower concentrations readily forms high  
49 viscous solution exhibiting pseudoplasticity [9]. Sodium alginate is an anionic polysaccharide  
50 derived from sea algae (Phaeophyceae) that contain 30–60 per cent of alginic acid. Sodium  
51 salt of alginic acid is a linear polymer made up of residues of 1, 4-linked D-mannuronic acid  
52 and D-guluronic acid [10]. Sodium alginate nanoparticles are also explored for designing  
53 pesticide delivery systems due to its biodegradability, biocompatibility, and low toxicity in  
54 nature. Therefore, the present study focuses on designing xanthan gum and sodium alginate  
55 based polymeric system for the delivery of diclosulam for improving weed control efficiency

## 56 **2. MATERIAL AND METHODS**

### 57 **2.1. Materials**

58 Sodium alginate (HiMedia: Cat No. RM7494) was purchased from HiMedia (Mumbai, India).  
59 IAMPURE Ingredients (Chennai, India) supplied xanthan gum. Calcium chloride anhydrous  
60 (Avra: Cat No. ASC2461)) was purchased from Avra Synthesis Private Limited. (Hyderabad,  
61 India), Phosphate buffer was procured from Molychem (Mumbai, India), Diclosulam herbicide  
62 (84% WDG) and ethanol were purchased locally. None of the chemicals was further purified  
63 before being employed in the study.

### 64 **2.2. Methods**

#### 65 **2.2.1. Encapsulation of diclosulam in Xanthan gum - Alginate microspheres**

66 Xanthan gum (XG) – Sodium alginate (SA) microspheres were prepared based on the earlier  
67 protocol [11] with some modifications through ionotropic gelation method. A homogeneous  
68 solution of xanthan gum and sodium alginate were prepared by dissolving in water using a  
69 reflux condenser at 45°C. The ratio of sodium alginate to xanthan gum was kept as 1:0.67 for  
70 the preparation of microspheres. The XG/SA mixture was dropped to ion gelation bath of  
71 calcium chloride (2, 4 and 6 per cent) to obtain microspheres. The distance between the  
72 delivery point of syringe and ionic solution was maintained at 7cm, while flow rate of polymer  
73 mixture was kept at 16 drops minute<sup>-1</sup>. Microspheres were cured in the gelation bath for 45  
74 minutes in the room temperature. Subsequently, microspheres were washed with deionized  
75 water to remove non-cross-linked cations over the surface of the beads. Beads were dried at  
76 room temperature for 48h until obtaining uniform weight of beads. Diclosulam was  
77 homogenized in the polymer matrix before dropping into gelation bath to facilitate the  
78 encapsulation of diclosulam in the polymeric systems.

79

#### 80 **2.2.2. Entrapment efficiency of Diclosulam in Microspheres**

81 Encapsulation efficiency represents the amount of active ingredient encapsulated in matrix  
82 complexes of xanthan gum-alginate polymeric systems. Herbicide loaded beads of varying  
83 concentrations were analyzed individually using UV-Vis spectrophotometer (Analytik Jena,  
84 Specord 210 Plus). Diclosulam (84 per cent WDG) was prepared to 10 ppm using 0.067 M  
85 phosphate buffer (6.8pH) for assessing the wavelength of maximum absorption through  
86 scanning with a wavelength of 200 to 800 nm in UV Vis spectroscopy. The known  
87 concentrations of diclosulam (5, 10, 15, 20, 25 and 30 ppm) standards were used to find OD  
88 values in UV Vis spectroscopy for obtaining standard curve. Similarly, microspheres (20 mg)  
89 containing diclosulam were dissolved in 10 ml of 0.067 M phosphate buffer (6.8 pH) for 4h  
90 complete dissolution of microspheres. Aliquot was filtered through membrane filter (0.22µm)  
91 to reduce the residual interaction and analyzed at  $\lambda_{max} = 251$  nm using a  
92 spectrophotometer. Diclosulam entrapment efficiency was calculated using the following  
93 formula

94 Encapsulation Efficiency (%) =  $\frac{\text{Actual herbicide content}}{\text{Theoretical herbicide content}} \times 100$

### 95 **2.2.3. Swelling behavior and water uptake of microspheres**

96 The swelling property and water uptake of diclosulam-loaded xanthan gum – alginate  
97 microspheres were assessed in terms of change in mass and diameter with function of time.  
98 Measurements of the initial diameter and mass of dried microspheres were made before  
99 beads were soaked for two hours at room temperature in phosphate buffer (6.8pH). The  
100 microspheres were retrieved from phosphate buffer in a regular intervals to assess mass and  
101 diameter at time 't'. The percent of water uptake and swelling per cent were calculated using  
102 following equations

103 Percent Swelling =  $\frac{\text{Diameter of microsphere at time "t" - Initial diameter of microsphere}}{\text{Initial diameter of microsphere}} \times 100$

104 Water uptake =  $\frac{\text{Weight of microsphere at time "t" - Initial weight of microsphere}}{\text{Initial weight of microsphere}} \times 100$

### 105 **2.2.4. Characterization of diclosulam loaded xanthan gum -alginate microspheres**

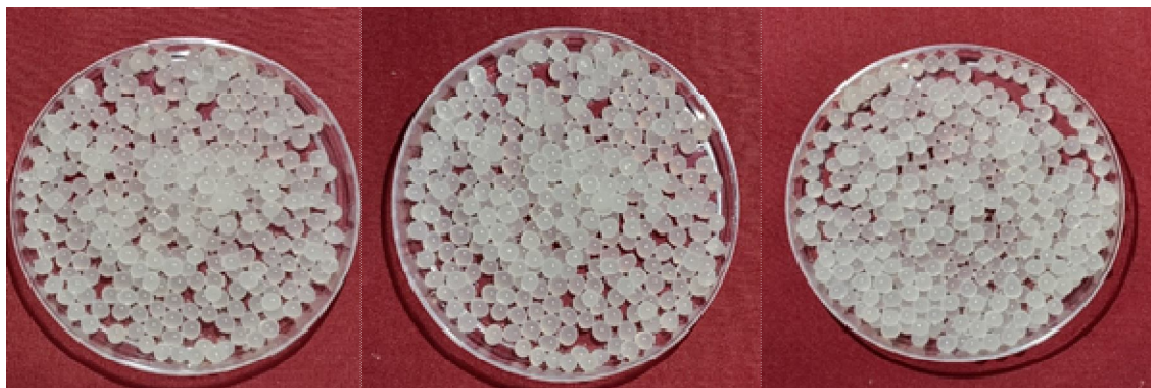
106 Diclosulam loaded xanthan gum – alginate microspheres were examined under digital  
107 optical fluorescent microscope (ProgRes C5 indi) at 5x magnification to determine the size of  
108 microsphere. The surface topography of microspheres was assessed using scanning  
109 electron microscope (Quanta 250, FEI, Czech Republic). Electron microscopy images were  
110 obtained by mounting the microsphere on carbon stub at an acceleration voltage of 10kV  
111 with chamber pressure of 1.0mm Hg. Fourier Transformed Infra-Red spectra of xanthan  
112 gum, sodium alginate, diclosulam, xanthan gum – alginate microsphere and diclosulam  
113 loaded xanthan gum – alginate microsphere was recorded using JASCO –FTIR-6800.

114 Attenuated total reflection (ATR) mode was used at wavenumber regime of 4000 to 400  $\text{cm}^{-1}$   
115 with 4  $\text{cm}^{-1}$  resolution and 32 scans. The pore size, pore radius and surface area of  
116 microspheres were assessed using Brunner –Emmet-Teller (QuantachromeNOVAtouch  
117 NT2LX-1). The microspheres were degassed at 100°C for 3h to remove moisture and  
118 subjected to the adsorption of nitrogen gas at series of pressure points (0 to 800 torr).

### 119 **3. RESULTS AND DISCUSSION**

120 Encapsulation of diclosulam in xanthan gum –sodium alginate polymeric microcapsules or  
121 microspheres was carried out through ionic gelation technique. The concentration of ion  
122 gelation bath affected the size and behaviour of xanthan gum–sodium alginate microspheres.  
123 Fresh and dried xanthan gum - sodium alginate microsphere without loading diclosulam  
124 cross-linked with various concentration of ion gelation bath (calcium chloride) are illustrated  
125 in Fig 1a, 1b, 1c and 2a, 2b and 2c. The microspheres were completely spherical in nature  
126 irrespective of ion gelation bath concentrations. Gelation occurs through ionic bonding  
127 between divalent cations in the gelation bath and carboxyl group of guluronic acids in sodium  
128 alginate and mannose units in xanthan gum. Gelation process results in the formation of  
129 three-dimensional structures, which further are stabilized through the exchange of sodium  
130 ions in the polymer matrix with divalent calcium ions in the gelation bath. The rate of divalent  
131 cations in gelation bath determines the sphericity of microspheres. The regain of spherical  
132 shape of polymer beads in the ion gelation bath occurs when the viscous force of polymers  
133 overcome the drag force of ion gelation bath [11]. Hence, the concentration of xanthan gum  
134 and sodium alginate used in the study creates viscous force to regain the spherical shape of  
135 beads through overcoming drag forces of ion gelation bath. Chloride ions interact with uronic  
136 acid of sodium alginate to form calcium alginate xanthan layer externally over the bead  
137 exchanging sodium ions. The digital fluorescence microscopic image of calcium chloride  
138 cross-linked xanthan gum-alginate microspheres shows a uniform undulation (black color)  
139 from periphery to center of the bead, which was cross-linked with two per cent of ion gelation  
140 bath (fig.3a). On the other hand, thick outer shell and smooth inner core were observed in  
141 beads cross-linked with, six per cent ion gelation bath (fig.3c). The wall materials surrounding  
142 the core molecules (herbicide) attribute to the greater improvement of physical and chemical  
143 stability and control the delivery of core materials [12, 13]. Matrix polymeric type delivery  
144 system (microspheres) offers the controlled release of core material through equidistant  
145 matrix erosion after a burst release at initial phase of delivery. Hence, the effects of calcium  
146 chloride concentrations (ionic cross linker) were observed in the digital images of fluorescent  
147 microscope. Higher rate of divalent ions complexes readily with peripheral layer of polymer  
148 matrix, thus resisting further penetration of divalent calcium into center of beads resulting in

149 poor crosslinking. Lower concentration of divalent ions in the gelation bath allows the  
150 movement of cations into beads completely to achieve higher crosslinking. The intensity of  
151 black coloration in the images indicates the intensity of calcium ions, where beads cross-  
152 linked with six per cent calcium chloride results in the thick black peripheral layer over the  
153 bead representing higher concentration of calcium ions and vice versa.



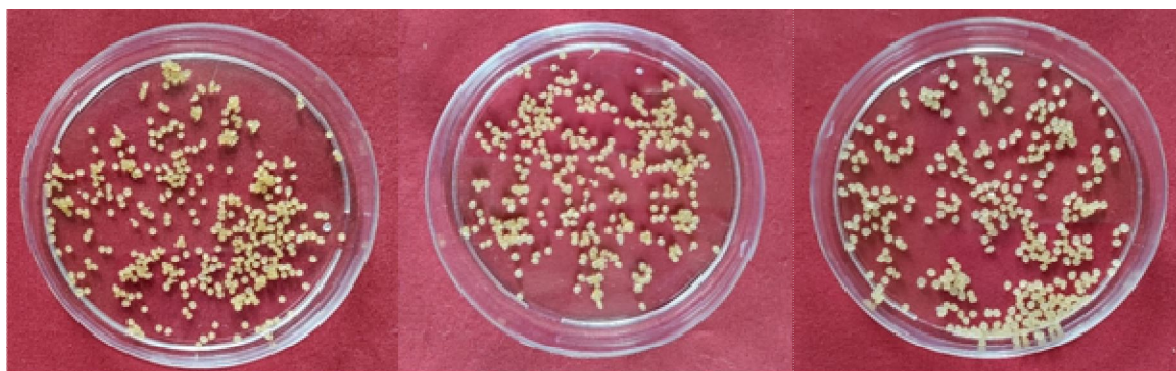
[1a]

[1b]

[1c]

154

155 **Fig1: Fresh Xanthan gum alginate microspheres: [1a]: 2% calcium chloride cross**  
156 **linked; [1b]: 4% calcium chloride cross linked; [1c]: 6% calcium chloride cross linked**



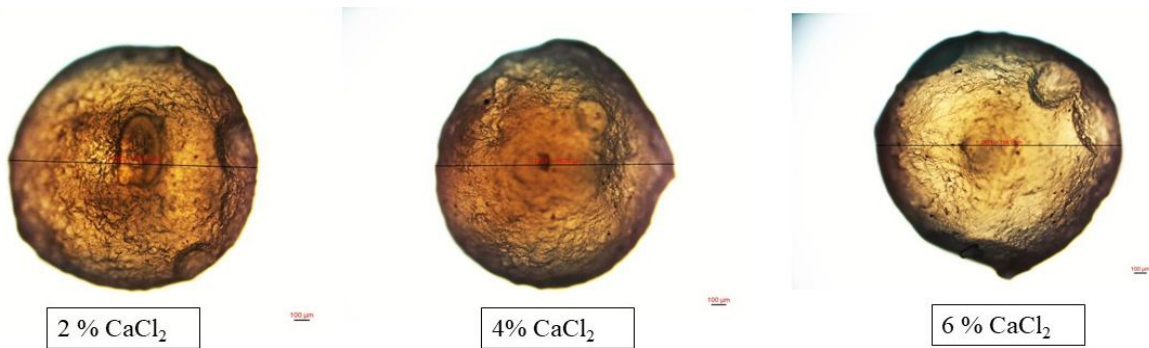
[2a]

[2b]

[2c]

157

158 **Fig2: Dried Xanthan gum alginate microspheres: [2a]: 2% calcium chloride cross**  
159 **linked; [2b]: 4% calcium chloride cross linked; [2c]: 6% calcium chloride cross linked.**

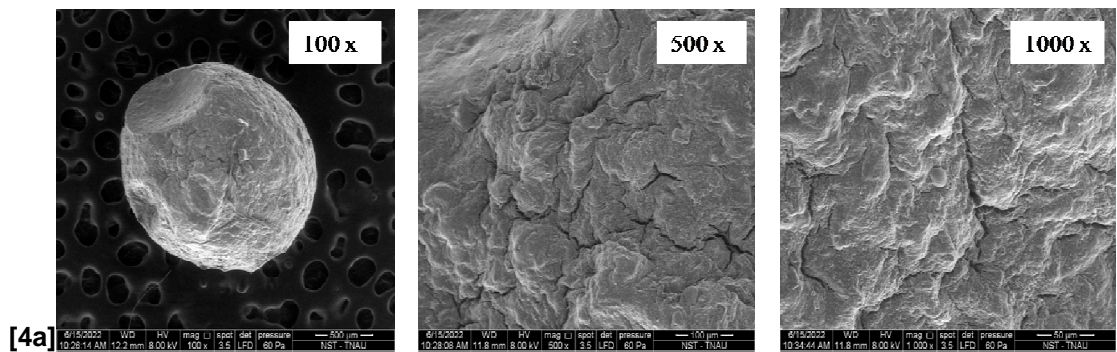


160  
161  
162  
163  
164  
165  
166  
167  
168  
169  
170  
171  
172  
173  
174  
175  
176  
177  
178

**Fig3: Digital optical fluorescent microscopic image of two, four and six percent Calcium chloride cross linked Xanthan gum – Alginate microsphere**

A uniform influx of calcium ions with efflux of water and sodium ions occurs at low concentration of ion gelation bath, whereas maximum cross-linking forms with higher concentration of calcium chloride at outer layer of polymer matrix (bead) that becomes hardened and prevents the further influx of calcium ions for cross linking, thus forming a smooth inner core.

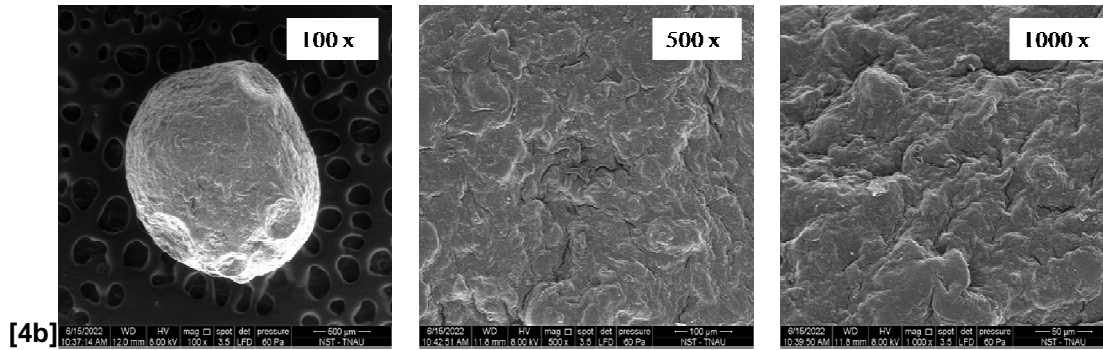
Scanning electron microscopic images of xanthan gum sodium alginate microspheres are illustrated in fig.4., which substantiate the above statement with a gradual decline in cracks or pinholes with increasing concentration of calcium ions in ion gelation bath. The shape and average diameter of xanthan gum-alginate microspheres are tabulated (Table1), which indicates the mean diameter of microsphere increases with increasing concentration of calcium chloride. Calcium ion influx, force efflux of water molecules and makes the microspheres to downsize resulting in smaller bead size at lower concentration of ion gelation bath. The mean diameter of beads, which were cross-linked, with concentration of six per cent calcium chloride resulted in larger bead size (2.00 mm) compared to beads (1.61 mm) cross-linked with two per cent concentration of calcium chloride.



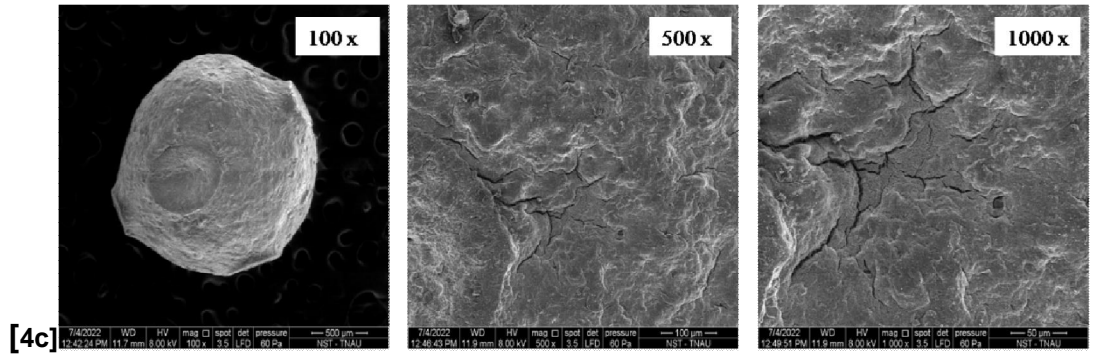
179

[4a]

180



181



182 **Fig4: SEM micrographs of Calcium chloride cross linked Xanthan gum-alginate**  
 183 **microsphere; [a]: 2% CaCl<sub>2</sub> Cross linked; [b]: 4% CaCl<sub>2</sub> Cross linked; [c]: 6% CaCl<sub>2</sub>**  
 184 **Cross linked.**

185 **Table1: Effect of various concentration of calcium chloride on mean diameter and**  
 186 **shape of xanthan gum alginate microspheres**

Concentration of Calcium chloride (%)	Diameter (mm)	Remarks
2 per cent	1.61	Beads were round and spherical
4 per cent	1.63	Beads were round and spherical
6 percent	2.00	Beads were oval

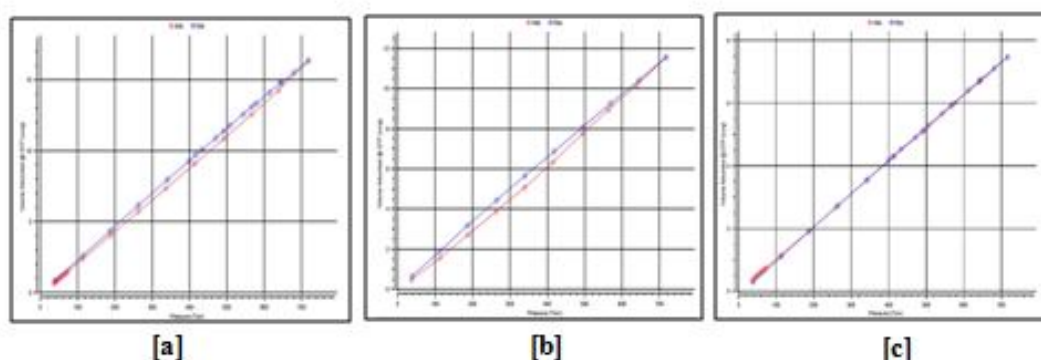
187 Pore volume and surface area governs the water uptake and dissolution of active molecules  
 188 loaded in the polymeric matrix system. Cross linking of polymers with different concentration  
 189 of ionic solution influence the surface area and pore volume of microspheres (Table 2). The  
 190 surface area (1.92 m<sup>2</sup> g<sup>-1</sup>) and pore radius (2.94 nm) of microspheres were higher with  
 191 crosslinking of two per cent calcium chloride, while beads complexed with six per cent  
 192 calcium chloride have less surface area (1.05 m<sup>2</sup> g<sup>-1</sup>) and pore radius (2.44 nm)

193 Thus, ionic solution concentration is inversely proportional to pore volume and surface area.  
 194 This implies that, a greater number of functional groups in polymers reacted at increasing  
 195 concentration of ionic solution resulting in increased bead size. Hence, downsizing of beads  
 196 with lower concentration of cross linkers proved with higher surface area, while uniform

197 crosslinking throughout the polymer matrix in lower concentration of calcium chloride  
 198 promotes higher pore radius. The type I isotherm (fig.5) of calcium chloride cross-linked  
 199 beads exhibits monolayer adsorption of gaseous molecules confirming the micro porous  
 200 nature of polymeric beads. Hence, the pore volume and surface area are foremost  
 201 parameter determining the release of core materials into the medium.

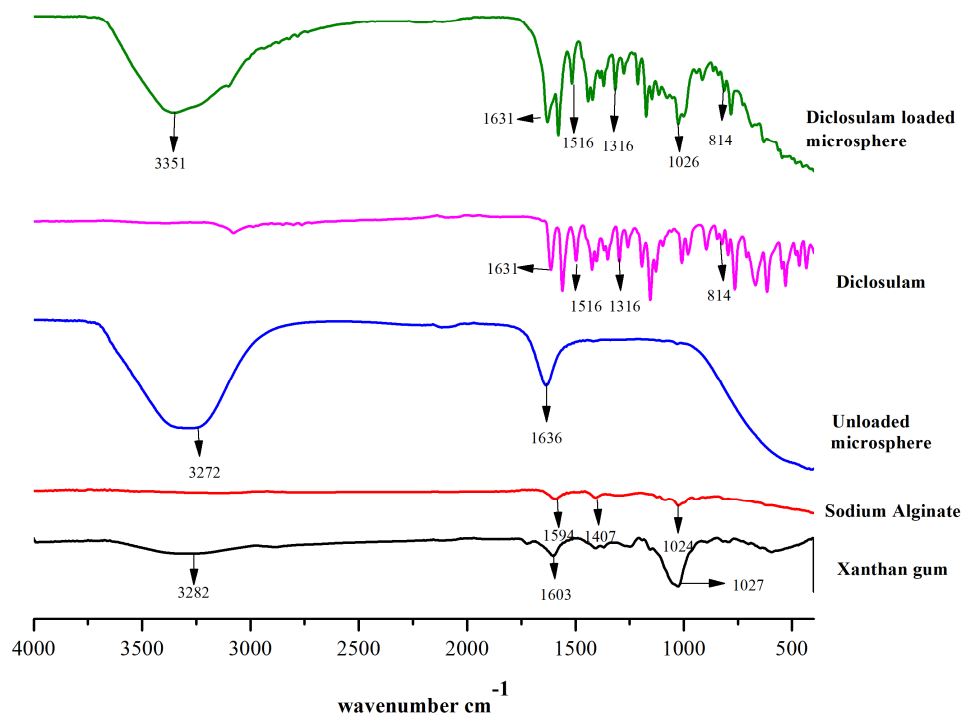
202 **Table 2: Effect of various concentrations of calcium chloride on pore volume, pore**  
 203 **radius and surface area of xanthan gum alginate microsphere.**

Treatments	Pore volume (cc/g)	Pore radius (nm)	Surface area (m <sup>2</sup> /g)
Calcium chloride 2%	0.024	2.94	1.92
Calcium chloride 4%	0.017	2.94	1.45
Calcium chloride 6%	0.011	2.44	1.05



204 **Fig5: Effect of Calcium chloride concentration on absolute isotherms of xanthan gum-**  
 205 **alginate microsphere.**

207 Further, diclosulam (hydrophobic moiety) was encapsulated in xanthan gum alginate  
 208 microspheres. The gelation of polymeric molecules entraps diclosulam simultaneously  
 209 through gelation with calcium divalent ions. Thus, ionic bond formed between calcium ions  
 210 and, carboxyl and hydroxyl groups of polymers favoring the formation of “egg box” complex  
 211 [14-17]. The three-dimensional structures get stabilized through exchanging sodium ions  
 212 with calcium ions in the polymeric system, provided maximum stability by minimizing internal  
 213 entropy [18], represented in the infra-red spectra of diclosulam loaded polymeric system (fig  
 214 6) forming strong bridging complex with disappearance of 1407cm<sup>-1</sup> peak corresponding to  
 215 OH bending of carboxylic acid.

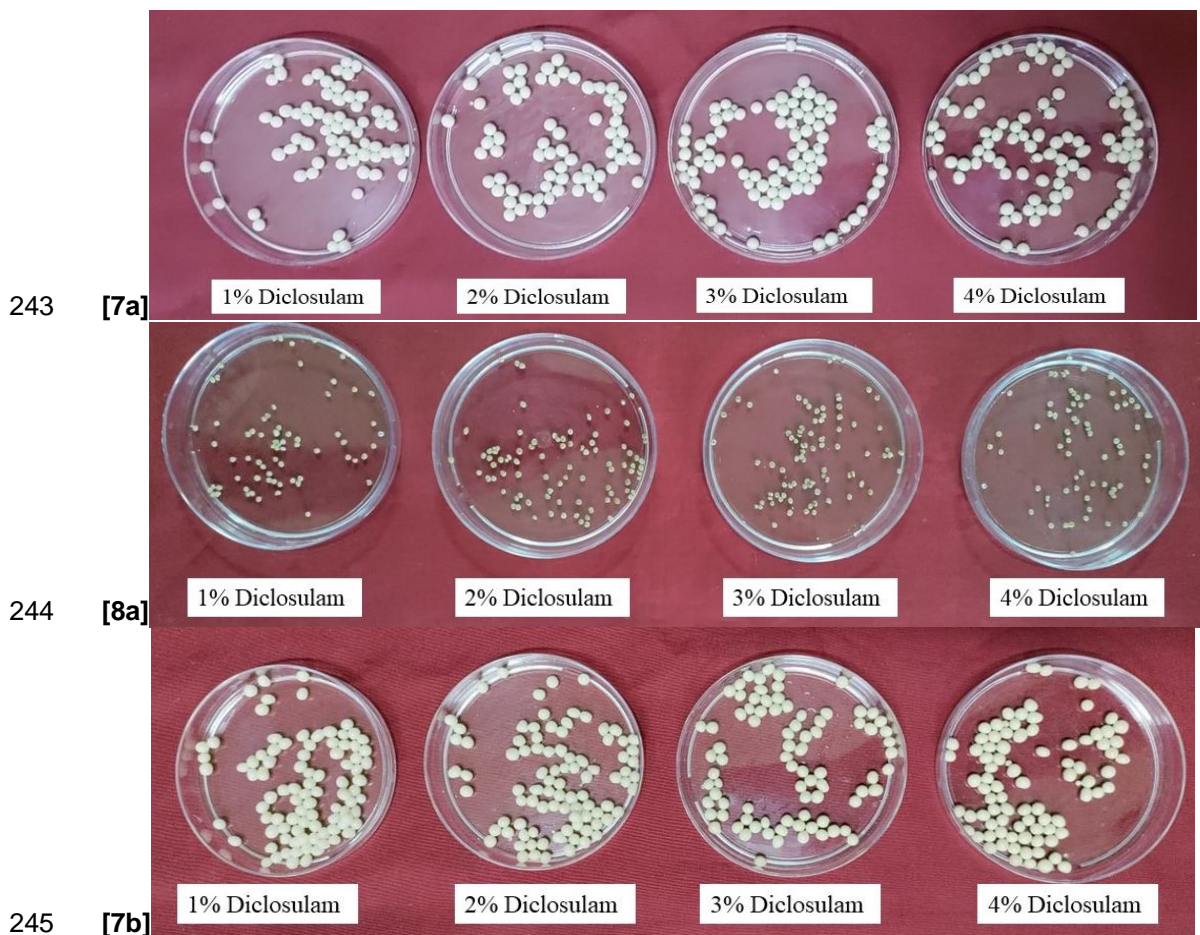


216

217 **Fig6: FTIR spectrum of xanthan gum, sodium alginate, xanthan gum – alginate**  
 218 **microsphere, diclosulam and diclosulam loaded xanthan gum – alginate microsphere**

219 The calcium ions offer instantaneous formation of bridging complex between carboxyl  
 220 groups of xanthan gum – sodium alginate polymeric system, indicates the formation of  
 221 partial covalent bond with decrease or disappearance of  $\text{COO}^-$  stretching peak at  $1024 \text{ cm}^{-1}$   
 222 of sodium alginate and shift to higher wavenumber  $1631 \text{ cm}^{-1}$  confirming the complexation  
 223 process in cross-linked polymeric system[19-21]. The intermolecular hydrogen bonding  
 224 formed between sodium alginate and xanthan gum was more prominent with an increased  
 225 intensity peak at  $3272 \text{ cm}^{-1}$  in the cross-linked polymeric system [22, 23]. The physical  
 226 adsorption of diclosulam to xanthan gum-alginate microspheres were confirmed through the  
 227 presence of characteristic vibrational peaks of 1578, 1516,850 to 550 corresponding to  
 228 crystalline nature and C-Cl stretching of halo compounds in diclosulam loaded polymeric  
 229 system (Fig 6). Different concentrations of diclosulam were loaded in xanthan gum alginate  
 230 microspheres. The fresh and dry beads of diclosulam loaded xanthan gum alginate  
 231 microspheres were shown in fig 7&8 respectively. The mean diameter of diclosulam loaded  
 232 xanthan gum-alginate microsphere increases with increasing concentration of diclosulam  
 233 (Table 3). Bead diameters of diclosulam-entrapped microspheres were increased with

234 concentration of diclosulam up to three per cent, whereas microspheres with four per cent of  
235 diclosulam resulted in lower size irrespective of concentration of ion gelation bath. Mean size  
236 of microspheres with one percent diclosulam was 2.12 mm, whereas the average diameter  
237 of beads with three per cent diclosulam was 2.30 mm. The size of microspheres with loading  
238 of diclosulam with four percent concentration was 2.10 mm, indicating the lesser size of  
239 beads with higher concentration of diclosulam beyond three per cent. Mass of diclosulam  
240 loaded microspheres increases gradually with increasing concentration of diclosulam.  
241 However, the discrepancy in mass and diameter of microspheres loaded with four per cent  
242 diclosulam might be due to the increased specific gravity of polymer solution.



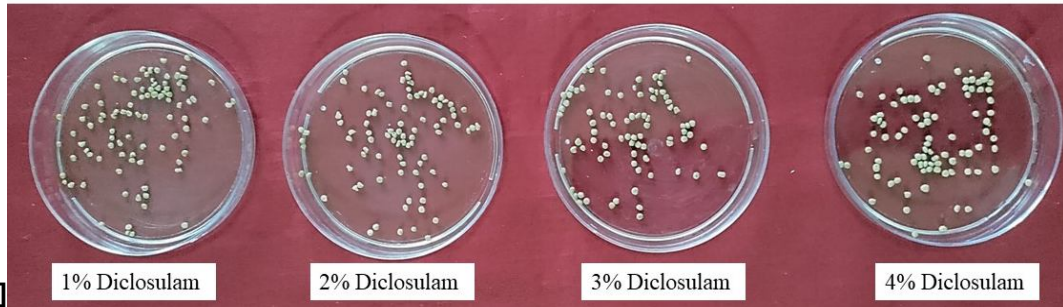
243 [7a]

244 [8a]

245 [7b]

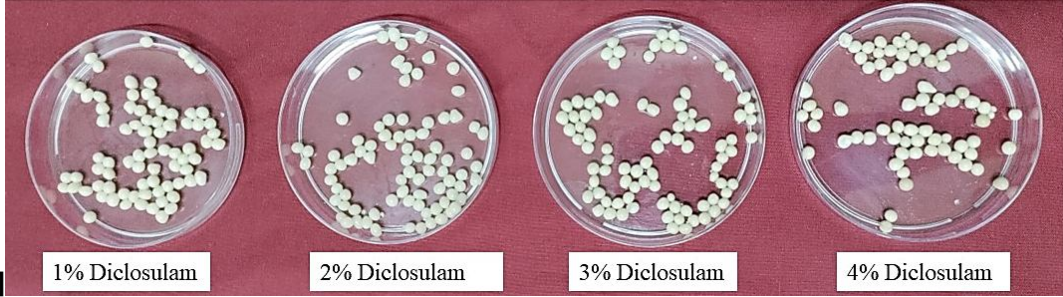
246

[8b]



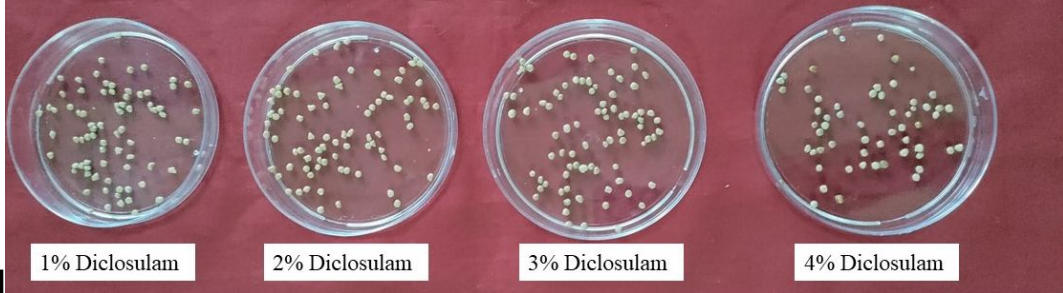
247

[7c]



248

[8c]

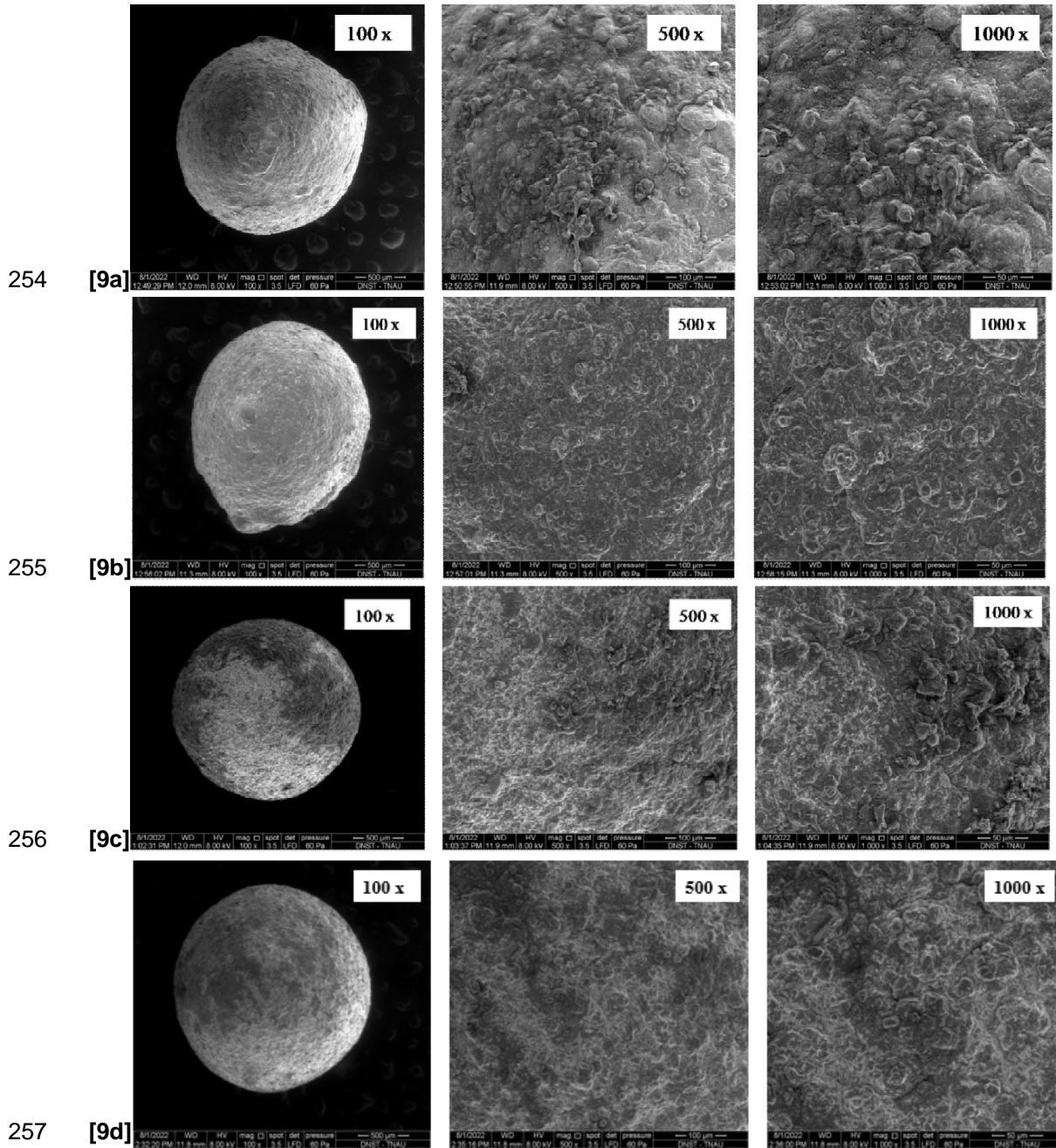


249 **Fig7&8: Diclosulam loaded Xanthan Gum-Alginate fresh and dry microsphere**  
 250 **respectively; [7a&8a]: 2% CaCl<sub>2</sub> crosslinked; [7b&8b]: 4% CaCl<sub>2</sub> Crosslinked; [7c&8c]:**  
 251 **6% CaCl<sub>2</sub> crosslinked**

252 **Table 3: Effect of calcium chloride and diclosulam concentrations on mean size and**  
 253 **shape of xanthan gum alginate microspheres**

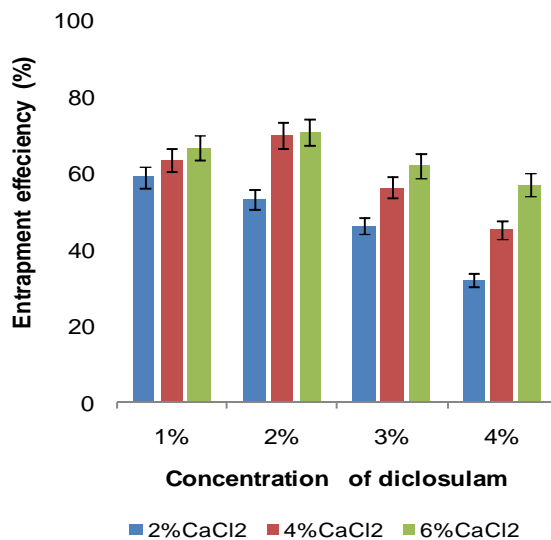
Calcium chloride	Diclosulam	Diameter (mm)	Remarks
2 percent	1 percent	1.99	Beads were round and spherical
	2 percent	2.16	Beads were round and spherical
	3 percent	2.26	Beads were round
	4 percent	2.02	Initially beads were round and turns oval upon increasing the gelation time
4 percent	1 percent	2.14	Beads were round and spherical
	2 percent	2.26	Beads were round and spherical
	3 percent	2.28	Beads were round
	4 percent	2.16	Initially beads were round and turns oval upon increasing the gelation time
6 percent	1 percent	2.25	Beads were round and spherical
	2 percent	2.27	Beads were round and spherical

3 percent	2.38	Beads were round
4 percent	2.13	Initially beads were round and turns oval upon increasing the gelation time



258 Fig9: SEM micrographs of diclosulam loaded in two percent calcium chloride  
 259 crosslinked xanthan gum alginate microsphere; [a] 1% Diclosulam loaded; [b]: 2%  
 260 Diclosulam loaded; [c]: 3% diclosulam loaded; [d]: 4% diclosulam loaded.

261 Scanning electron microscopic images of diclosulam loaded polymeric system revealed that,  
 262 appearance of fringes of xanthan gum – alginate microspheres and exhibition of protrusions  
 263 over the surface of microspheres forming an undulated surface which signifies the presence  
 264 of particulate matter. The intensity of particulate matter increases with increasing  
 265 concentration of diclosulam (fig 9) loaded in the polymeric system. A comparison of  
 266 entrapment efficiency of various concentration of diclosulam loaded in xanthan gum –  
 267 alginate microsphere was shown in fig 10. The entrapment efficiency of diclosulam  
 268 decreases with increasing concentration of diclosulam in xanthan gum alginate  
 269 microspheres. The higher concentration of diclosulam increases the polymer to drug ratio,  
 270 thereby it reaches saturation and declines the entrapment efficiency. Higher entrapment  
 271 efficiency (69.6 and 70.3 per cent) of diclosulam was noticed in six percent and four percent  
 272 calcium cross linked microspheres loaded with two percent diclosulam followed by two per  
 273 cent calcium cross linked microspheres with one per cent diclosulam with an entrapment  
 274 efficiency of 58.6 per cent. The lowest entrapment efficiency was observed in microspheres  
 275 with loading of diclosulam @ four per cent, might be due to efflux of diclosulam molecules out  
 276 of polymeric system to achieve equilibrium diffusion coefficient with surrounding ion gelation  
 277 bath. Conversely, [24, 25] reported that, entrapment efficiency decreases with increasing  
 278 concentration of crosslinkers.



279

280 **Fig10: Effect of calcium chloride and diclosulam concentration on entrapment**  
 281 **efficiency of diclosulam in Xanthan gum alginate microsphere**

282 Water uptake in the polymeric systems determines release kinetics of entrapped functional  
 283 materials. The effect of various concentrations of calcium chloride on water uptake of  
 284 diclosulam-loaded microspheres was shown in fig.11. The percent of water uptake increases

285 with time in microspheres with irrespective cross linker concentration. The higher water  
286 uptake was observed at 35<sup>th</sup> minute in microspheres cross-linked with two per cent  
287 concentration of calcium chloride followed by four per cent. However, microspheres formed  
288 with six per cent calcium chloride get dissipated in water medium within 10 minutes of  
289 incubation.

290 [a]

291 [b]

292 [c]

293 **Fig11: Effect of different concentration of calcium chloride on water uptake of**  
294 **diclosulam loaded (1%, 2%, 3% & 4%) and unloaded xanthan gum-alginate**  
295 **microsphere; [a]: 2% CaCl<sub>2</sub> crosslinked; [b]:4% CaCl<sub>2</sub> crosslinked; [c]: 6% CaCl<sub>2</sub>**  
296 **crosslinked**

297 Lesser water uptake in microspheres cross-linked with six per cent of calcium chloride was  
298 due to high degree of cross-linking over the surface. Swelling studies of microspheres  
299 indicated that beads cross-linked with lesser concentration of calcium chloride (2 and 4 per  
300 cent) absorbs water and reached maximum uptake of water during 30 to 35 minutes of  
301 incubation, while microspheres with six per cent attained maximum water uptake with 10  
302 minutes of incubation. Slower water influx was observed in the polymeric microsphere matrix  
303 formed with lesser concentration of calcium during the initial phase of incubation and  
304 reaches saturation with completely disintegrated microsphere polymer. Microspheres cross  
305 linked with higher concentration of calcium attain saturation rapidly and dissolve with burst  
306 release of functional molecule through poorly crosslinked core region [26].

#### 307 **4. CONCLUSION**

308 This study revealed that calcium mediated ionotropic gelation of xanthan gum-alginate  
309 composite resulted in spherical and stable beads possessing ability for the sustained release  
310 of diclosulam. The mean diameter of xanthan gum microsphere increased from 1.61mm to  
311 2.00 mm with increasing concentration of calcium ions in gelation bath. The entrapment  
312 efficiency of diclosulam @ two percent was higher with crosslinking of 4 and 6 per cent  
313 calcium gelation bath, however, microspheres cross-linked with higher concentration + in  
314 water medium. The microspheres with lower cross linker concentration offers controlled  
315 release of active molecules, which proved from the water uptake studies. Burst releases of

316 mechanism of microspheres are not for the delivery of diclosulam herbicide due to localized  
317 release of diclosulam from microspheres that induces phytotoxicity. Microspheres cross-  
318 linked with two and four per cent calcium chloride offers controlled release of diclosulam,  
319 which synchronize with crop growth duration, will not cause phytotoxicity in crops and  
320 achieve prolonged weed control.

## 321 **ACKNOWLEDGEMENTS**

322 All authors acknowledged the Department of Nano Science & Technology and Department of  
323 Agronomy for availing the infrastructure to carry out the experiment in Tamil Nadu  
324 Agricultural University.

## 325 **COMPETING INTERESTS**

326 Authors have declared that no competing interest exists.

327

## 328 **REFERENCES**

329

- 330 1. Sunitha, N. and D.L. Kalyani, Weed management in maize (*Zea mays* L.)-a review.  
331 *Agricultural Reviews* 2012; 33(1).
- 332 2. Kumar, B.N., et al., Weed management in groundnut with new herbicide molecules.  
333 *Indian Journal of Weed Science* 2019; 51(3): 306-307.
- 334 3. Aktar, W., D. Sengupta, and A. Chowdhury, Impact of pesticides use in agriculture:  
335 their benefits and hazards. *Interdisciplinary toxicology* 2009; 2(1): 1-12.
- 336 4. Pavithran, P., et al., Synthesis and Characterization of Pectin Beads for the Smart  
337 Delivery of Agrochemicals. 2021.
- 338 5. Pandey, S. and S.B. Mishra, Graft copolymerization of ethylacrylate onto xanthan  
339 gum, using potassium peroxydisulfate as an initiator. *International journal of*  
340 *biological macromolecules* 2011; 49(4): 527-535.
- 341 6. Petri, D.F., Xanthan gum: A versatile biopolymer for biomedical and technological  
342 applications. *Journal of Applied Polymer Science* 2015; 132(23).
- 343 7. Rajeswari, K.R., et al., Development and characterization of valsartan loaded  
344 hydrogel beads. *Der Pharmacia Lettre* 2012; 4: 1044-1053.
- 345 8. Cortes, H., et al., Xanthan gum in drug release. *Cellular and Molecular Biology*  
346 2020; 66(4): 199-207.
- 347 9. Lopes, B.d.M., et al., Xanthan gum: properties, production conditions, quality and  
348 economic perspective. *Journal of Food and Nutrition Research*. 2015; 54(3): 185-  
349 194.
- 350 10. Choudhary, R.C., et al., *Chitosan nanomaterials for smart delivery of bioactive*  
351 *compounds in agriculture*, in *Nanoscale engineering in agricultural management*.  
352 2019, CRC Press. p. 124-139.
- 353 11. Pongjanyakul, T. and S. Puttipipatkachorn, Xanthan–alginate composite gel beads:  
354 molecular interaction and in vitro characterization. *International Journal of*  
355 *Pharmaceutics* 2007; 331(1): 61-71.
- 356 12. Bannikova, A., et al., Microencapsulation of fish oil with alginate: In-vitro evaluation  
357 and controlled release. *LWT* 2018; 90: 310-315.
- 358 13. Menin, A., et al., Effects of microencapsulation by ionic gelation on the oxidative  
359 stability of flaxseed oil. *Food Chemistry* 2018; 269: 293-299.

- 360 14. Banerjee, A., D. Nayak, and S. Lahiri, A new method of synthesis of iron doped  
361 calcium alginate beads and determination of iron content by radiometric method.  
362 Biochemical Engineering Journal 2007; 33(3): 260-262.
- 363 15. Chandy, T., D.L. Mooradian, and G.H. Rao, Evaluation of modified  
364 alginate-chitosan-polyethylene glycol microcapsules for cell encapsulation. Artificial  
365 organs 1999; 23(10): 894-903.
- 366 16. Leick, S., et al., Deformation of liquid-filled calcium alginate capsules in a spinning  
367 drop apparatus. Physical Chemistry Chemical Physics 2010; 12(12): 2950-2958.
- 368 17. Martinsen, A., I. Storrø, and G. Skjærk-Bræk, Alginate as immobilization material: III.  
369 Diffusional properties. Biotechnology and bioengineering 1992; 39(2): 186-194.
- 370 18. Nunes, R. and E. Rotstein, Thermodynamics of the water-foodstuff equilibrium.  
371 Drying Technology 1991; 9(1): 113-137.
- 372 19. Nakanishi, K. and P.H. Solomon, *Infrared absorption spectroscopy*. 1977: Holden-  
373 day.
- 374 20. Wanchoo, R. and P. Sharma, Viscometric study on the compatibility of some water-  
375 soluble polymer-polymer mixtures. European Polymer Journal 2003; 39(7): 1481-  
376 1490.
- 377 21. Tang, C.Y., Z. Huang, and H.C. Allen, Binding of Mg<sup>2+</sup> and Ca<sup>2+</sup> to palmitic acid  
378 and deprotonation of the COOH headgroup studied by vibrational sum frequency  
379 generation spectroscopy. The Journal of Physical Chemistry B 2010; 114(51):  
380 17068-17076.
- 381 22. Puttipipatkachorn, S., T. Pongjanyakul, and A. Priprem, Molecular interaction in  
382 alginate beads reinforced with sodium starch glycolate or magnesium aluminum  
383 silicate, and their physical characteristics. International journal of pharmaceutics  
384 2005; 293(1-2): 51-62.
- 385 23. Sartori, C., et al., Determination of the cation content of alginate thin films by FTi. r.  
386 spectroscopy. Polymer 1997; 38(1): 43-51.
- 387 24. Singh, B.N. and K.H. Kim, Effects of divalent cations on drug encapsulation  
388 efficiency of deacylated gellan gum. Journal of microencapsulation 2005; 22(7): 761-  
389 771.
- 390 25. Maiti, S., et al., Tailoring of locust bean gum and development of hydrogel beads for  
391 controlled oral delivery of glipizide. Drug Delivery 2010; 17(5): 288-300.
- 392 26. Sugawara, S., T. Imai, and M. Otagiri, The controlled release of prednisolone using  
393 alginate gel. Pharmaceutical research 1994; 11(2): 272-277.